PAPER

Channel Arrangement Design in Lumped Amplified WDM Transmission over NZ-DSF Link with Nonlinearity Mitigation Using Optical Phase Conjugation

Shimpei SHIMIZU[†a)], **Takayuki KOBAYASHI**[†], **Takeshi UMEKI**[†,††], **Takushi KAZAMA**[†,††], **Koji ENBUTSU**[††], ***Members***, **Ryoichi KASAHARA**[††], ***Senior Member***, ***and*** **Yutaka MIYAMOTO**[†], ***Fellow***

SUMMARY Optical phase conjugation (OPC) is an all-optical signal processing technique for mitigating fiber nonlinearity and is promising for building cost-efficient fiber networks with few optic-electric-optic conversions and long amplification spacing. In lumped amplified systems, OPC has a little nonlinearity mitigation efficiency for nonlinear distortion induced by cross-phase modulation (XPM) due to the asymmetry of power and chromatic dispersion (CD) maps during propagation in transmission fiber. In addition, the walk-off of XPM-induced noise becomes small due to the CD compensation effect of OPC, so the deterministic nonlinear distortion increases. Therefore, lumped amplified transmission systems with OPC are more sensitive to channel spacing than conventional systems. In this paper, we show the channel spacing dependence of NZ-DSF transmission using amplification repeater with OPC. Numerical simulations show comprehensive characteristics between channel spacing and CD in a 100-Gbps/λ WDM signal. An experimental verification using periodically poled $LiNbO_3$-based OPC is also performed. These results suggest that channel spacing design is more important in OPC-assisted systems than in conventional dispersion-unmanaged systems.

key words: *optical signal processing techniques for optical communications, optical phase conjugation, nonlinear optics, periodically poled $LiNbO_3$ waveguide*

1. Introduction

Digital coherent technologies have increased the transmission capacity and distance in optical fiber communication systems. It is possible to compensate for linear impairments such as chromatic dispersion (CD) and polarization-mode dispersion (PMD) with digital signal processing (DSP) in digital coherent transmission. 100-Gbps/ch. wavelength-division multiplexing (WDM) transmission systems using dual-polarized quadrature-phase-shift keying (DP-QPSK) are widely deployed in core and metro fiber networks [1]. When constructing cost-efficient long-haul fiber networks, it is important that the spacing of repeaters based on optic-electric-optic conversion and optical amplification is extended. One of the factors restricting the repeater spacing is fiber nonlinearities such as self-phase modulation (SPM), cross-phase modulation (XPM), and four-wave mixing (FWM) caused by optical the Kerr-effect [2]. These nonlinearities cause there to be phase noise in the signal and the signal-to-noise ratio (SNR) to deteriorate. As the fiber-input power increases, the optical SNR (OSNR) improves. However, the optical signal is strongly distorted due to fiber nonlinearities when the power exceeds a specific value. Thus, conventional optical transmission systems are operated with the optimal fiber-input power balanced between OSNR-improvement and signal distortion due to fiber nonlinearities. Although techniques for digitally mitigating fiber nonlinearity, such as digital back propagation [3], the Volterra equalizer [4], and the neural-network-based equalizer [5], have been developed, the deployment of novel transponders with these functions is required.

Optical phase conjugation (OPC) is one of the all-optical signal processing techniques for mitigating nonlinear distortion [6]–[10]. By using the OPC with the existing optical nodes, the SNR can be improved. In the OPC-assisted systems, signal light is converted to phase-conjugated light at the center of two spans in a transmission link. Nonlinear distortion and CD generated in a span before OPC are canceled by those generated in a span after OPC. OPC is generally conducted by utilizing an optical parametric amplification (OPA) process in highly nonlinear media such as highly nonlinear optical fibers (HNLF) and periodically poled $LiNbO_3$ (PPLN) waveguides. In the frequency non-degenerate OPA process, phase-conjugated light, namely idler light, is generated at a frequency different from that of signal light due to the nonlinear interaction between signal and pump light. In particular, the idler generation process in $\chi^{(2)}$-nonlinear media is called differential frequency generation (DFG). Phase rotation due to fiber nonlinearity and CD is mitigated with the propagation of phase-conjugated light. For complete compensation of nonlinear distortion, the nonlinear phase rotations that occur in the span before and after OPC must be the same. Therefore, the performance of nonlinearity mitigation with OPC depends on the symmetry of an optical power map and a CD map during propagation between two spans [7]. When constructing a symmetrical transmission link, distributed Raman amplification (DRA) is effective. The combination of DRA and OPC has demonstrated an improvement in nonlinear tolerance in long-haul fiber transmission [8]–[10]. On the other hand, enhancing the nonlinear mitigation efficiency of OPC in lumped amplified systems is

Manuscript received October 29, 2021.
Manuscript revised December 15, 2021.
Manuscript publicized January 17, 2022.

[†]The authors are with NTT Network Innovation Labs., NTT Corporation, Yokosuka-shi, 239-0847 Japan.
[††]The authors are with NTT Device Technology Labs., NTT Corporation, Atsugi-shi, 243-0198 Japan.
a) E-mail: shimpei.shimizu.ge@hco.ntt.co.jp

DOI: 10.1587/transcom.2021EBP3179

an important issue. So far, it has been shown that mitigation, especially for XPM, is particularly small in lumped amplified transmission [11]. For enhancement of nonlinearity mitigation in lumped amplified systems, optimizing the CD map by pre-dispersion loading in accordance with the asymmetry with a power map has been demonstrated [12], [13].

Generally, in a dispersion-unmanaged transmission link, XPM-induced noise is not dominant thanks to the walk-off effect. Even if the channel spacing, which affects the efficiency of XPM-induced noise, is widened, a large improvement in nonlinear tolerance cannot be obtained. In an OPC-assisted system, the walk-off becomes small because the CD of the propagating light fluctuates around zero due to the CD compensation effect of OPC, similar to a periodically dispersion-managed link. Therefore, OPC-assisted systems are more sensitive to channel spacing, so a wider channel spacing will be effective in improving the transmission performance in comparison with no-OPC systems. However, the effects of channel spacing in digital coherent WDM transmission systems with OPC have not been fully investigated. In this paper, we investigate channel arrangement design for WDM transmission systems using lumped amplification repeaters with OPC. In particular, we focus on a transmission link consisting of non-zero dispersion-shift fibers (NZ-DSFs) that is particularly affected by XPM. First, we perform numerical simulations using the split-step Fourier method (SSFM) to evaluate the impact of XPM on OPC-assisted systems. The effect of OPC on improving the SNR is comprehensively characterized by varying the channel spacing and CD. Next, experiments with long-haul transmission over an NZ-DSF link where the channel spacing is 100, 200, or 400 GHz are conducted using PPLN-based OPC to verify the validity of the simulation results. We demonstrate that the impact of XPM is larger in the OPC-assisted system than the conventional dispersion-unmanaged system, and the transmission performance can be greatly enhanced by extending the channel spacing.

2. Link Design Strategy with OPC in Lumped Optical Amplified WDM Transmission

The generation efficiency of nonlinear distortion due to XPM depends on the difference in the propagation constant $\Delta\beta$ between the interacting components. With a large $\Delta\beta$, the noise property of the XPM-induced phase rotation becomes small thanks to a strong walk-off effect. Extending the channel spacing is effective in increasing $\Delta\beta$ between interacting channels. Therefore, CD and WDM spacing are important parameters in transmission link design, and the walk-off length of nonlinear distortion caused by XPM is well-known as:

$$L_w = \frac{T}{|D\Delta\lambda|} \tag{1}$$

where T is the symbol interval, D is the second-order CD coefficient of a transmission link, and $\Delta\lambda$ is the wavelength separation between interacting components [14].

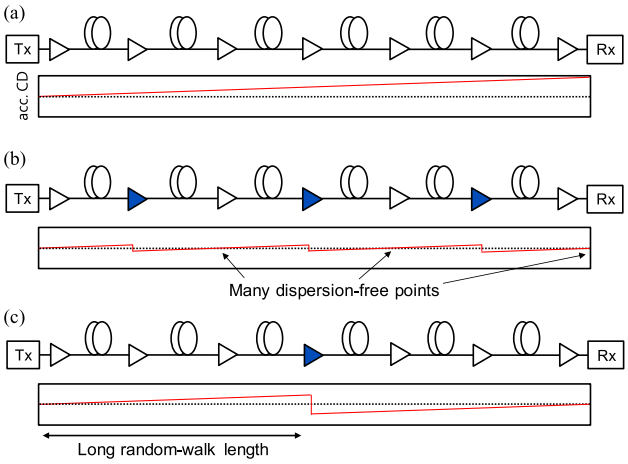

Fig. 1 System configurations and accumulated CD (red lines) of six-spans transmission (a) without OPC, (b) with three OPC insertions, and (c) with one OPC insertion. Blue and white triangles indicate lumped inline amplifiers with and without OPC, respectively.

Figure 1 shows an example of the lumped amplified transmission systems and CD maps with and without OPC. In the case without OPC, CD accumulates linearly and leads to walk-off in nonlinear distortion, especially induced by XPM. On such a dispersion-unmanaged link, transmission performance is less dependent on channel spacing because SPM is a dominant factor to nonlinear distortion. In contrast, signal light is propagated without CD accumulating in OPC-assisted systems. Because there is a small walk-off due to there being many dispersion-free points [Fig. 1(b)], the total nonlinearity in the entire system is larger than the no-OPC system, similar to a periodically dispersion-managed link. On the other hand, nonlinear phase rotations before and after OPC occur in directions counter each other. Therefore, the accumulated nonlinear-phase noise in the received signal depends on the balance between the enhancement of nonlinearity due to the small walk-off and the cancellation of opposing phase rotations. As shown in Fig. 1(c), it is possible to increase the walk-off effect in XPM by reducing the number of OPC insertions [11]. However, the compensation performance for the non-deterministic nonlinearity with a random-walk property caused by PMD and signal-noise nonlinear interaction deteriorates due to the longer OPC interval [15], [16]. Therefore, the random fluctuation in the received signal quality becomes large. In the following, we focus on the case of inserting OPC every two spans as shown in Fig. 1(b).

The mitigation effect of nonlinear-phase noise depends on the symmetry in the transmission conditions (CD map and power map) before and after OPC. Ignoring the dispersion slope of the transmission fiber and frequency shift due to OPC, the symmetry of the power map is important because the CD map is naturally symmetric by OPC insertions. Therefore, the utilization of distributed amplification is effective. However, in lumped amplified systems, there is no other way but to reduce the span length and loss to construct a symmetrical power map. The asymmetry of the

transmission conditions causes deterioration in the mitigation efficiency of nonlinear-phase noise, especially induced by XPM. In addition, OPC has a strong mitigation effect on SPM-induced noise, which is a nonlinear distortion in a narrow band such that does not depend much on the symmetry of the power and CD maps. Therefore, XPM becomes a dominant factor to nonlinear distortion by inserting OPC. The efficiency of XPM-induced phase noise is dependent not on only CD accumulation but also on the channel spacing. Therefore, OPC-assisted systems, which have a small walk-off for XPM-induced noise, are more sensitive to the channel spacing than no-OPC systems. Also, this effect is particularly noticeable in the case of a small CD transmission link consisting of NZ-DSFs. This characteristic is similar to WDM transmission using digital backpropagation, which generally has the capability to compensate only for nonlinear phase noise induced by SPM [17]. From the above, it is considered that the extension of the channel spacing is effective in improving the transmission performance in the OPC-assisted system. In the following sections, changes in nonlinear tolerance with respect to channel spacing and CD are discussed with numerical simulations and long-haul transmission experiments.

3. Numerical Simulation for 12 × 80-km Five-Channel WDM Transmission over NZ-DSF with Loss-Less OPC

As mentioned above, channel spacing will be important in OPC-assisted systems. In this section, we perform numerical simulations to investigate the design of the channel arrangement for lumped amplified transmission systems with OPC. It was assumed that there was no loss and gain when the WDM signal passed through OPC in order to confirm only the change in nonlinearity caused by the insertion of OPC.

3.1 Simulation Model

Figure 2 shows a simulation model. Optical fibers with a small CD such as NZ-DSFs were assumed as a transmission line. On the transmitter side, five-channel 100-Gbps/λ WDM signal were generated using Nyquist-pulse-shaped 32-Gbaud DP-QPSK with a 0.1-roll-off factor. The WDM channel spacing was set to 100, 200, or 400 GHz. In this simulation, only five channels were simulated due to computational resources, but in reality, 10 channels could be implemented using OPC with a complementary spectral inversion configuration [5]. The transmission link consisted of 12 × 80-km NZ-DSFs and inline erbium-doped fiber amplifiers (EDFAs). Thus, 960-km lumped amplified transmission was simulated. During this 960-km transmission, OPC was inserted every two spans. The propagation in the NZ-DSFs was simulated on the basis of the nonlinear Schrödinger equation (NLSE) considering a CD up to the third order calculated by the SSFM. The parameters were as follows. The dispersion slope was 0.07 ps/nm^2/km, the propagation loss was 0.23 dB/km, the nonlinear optical constant was 2.3 /W/km,

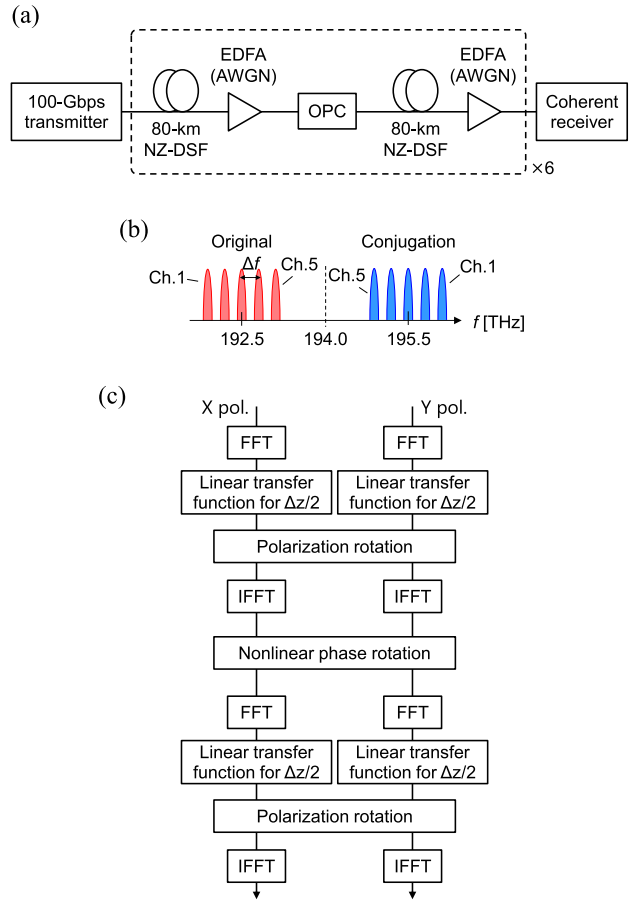

Fig. 2 Simulation model. (a) Configuration of transmission system with loss-less OPC. (b) Channel arrangement of five-channel WDM signal. Channel spacing Δf is 100, 200, or 400 GHz. (c) Simulation flow per Δz of SSFM. (I) FFT: (inverse) fast Fourier transform.

the PMD coefficient was 0.1 ps/km$^{1/2}$, the noise figure (NF) of the inline EDFAs was 4.5 dB, the center frequency of the WDM signal was 192.5 THz, and the center frequency of the phase-matching of the nonlinear medium used for OPC was 194.0 THz. The local CD at 1550 nm (193.4 THz) was varied from −3.0 to 6.0 ps/nm/km in 0.5-ps/nm/km increments. The propagation step size Δz in the SSFM was set adaptively in accordance with the power of the propagating light so that the calculation error of the nonlinear phase rotation was less than 0.1% [3], [18]. After passing through OPC, the center frequency of the WDM signal was converted to 195.5 THz. The CDs before and after OPC was set to different values calculated in accordance with the dispersion slope, the local CD at 1550 nm, and the center frequency of the WDM signal. Figure 2(c) shows the simulation flow per Δz of the SSFM. The linear transfer effect, which consisted of propagation loss and CD, of each polarization component was calculated independently, and random polarization rotation and PMD were applied in the frequency domain. After that, nonlinear phase rotation was applied in the time domain. The amount of nonlinear phase rotation was calculated by using the sum of the instant power for each polarization component. In the

EDFA section, additive white Gaussian noise (AWGN) with a 4.5-dB NF was added to the signal after the compensation for propagation loss. The root-mean square (RMS) of the amplitude in a one-phase component of AWGN is expressed as

$$n_{RMS} = \sqrt{\frac{a_{NF}(G-1)h\nu}{4}\Delta f} \tag{2}$$

where a_{NF} is the NF of an inline amplifier, G is the gain of EDFA, h is the Plank constant, ν is the center frequency of the WDM signal, and Δf is the bandwidth of the analysis area. After calculating the 12×80-km transmission, the WDM signal was frequency-shifted so that the tested channel was at the center of the analysis area, and it was then extracted with a low-pass filter. The extracted channel was demodulated using a 2×2 adaptive filter updated by the decision-directed least-mean square (DD-LMS) algorithm after CD compensation. The signal quality was evaluated by calculating the SNR on the basis of the variance in the signal after the symbol decision from the desired symbols.

3.2 Results and Discussion

Figure 3 shows simulation results for the SNR of the center channel as a function of the input power with 3.0-ps/nm/km local CD at 1550 nm. It was confirmed that the power tolerance was also improved by OPC regardless of the channel spacing. In the no-OPC cases, the improvement in power tolerance from extending the channel spacing was small. The reason for this is that the effect of XPM was not that great due to the walk-off from the accumulated CD even in the 100-GHz spacing. SPM-induced noise was dominant in the nonlinear distortion. The SNR difference at the optimal power between the 100-GHz spacing and 400-GHz spacing was 0.43 dB, and the optimal input power was −2 dBm/ch. regardless of the channel spacing. The OPC-assisted systems showed a larger improvement in power tolerance with an extended channel spacing than the no-OPC systems because they were strongly affected by XPM-induced noise due to the small walk-off. SPM-induced noise was efficiently mitigated by the insertion of OPC, XPM became a major factor to nonlinear distortion. The SNR difference at the optimal power between the 100-GHz spacing and 400-GHz spacing was 1.79 dB. The optimal input power increased by 1 dBm as the channel spacing increased. The amount of SNR improvement thanks to the nonlinearity mitigation by OPC for each channel spacing was 1.17 dB with 100 GHz, 1.78 dB with 200 GHz, and 2.52 dB with 400 GHz. As shown from these results, since the influence of the channel spacing was large in the transmission system using OPC, it is necessary to design the channel spacing more carefully on the basis of the required number of channels.

Figure 4 shows the channel dependence of SNR at the optimal power with a local CD of 3.0 ps/nm/km. The channel numbers were arranged in ascending order of frequency from the smallest channel number. It has been reported that the frequency dependence of the nonlinear mitigation effect for

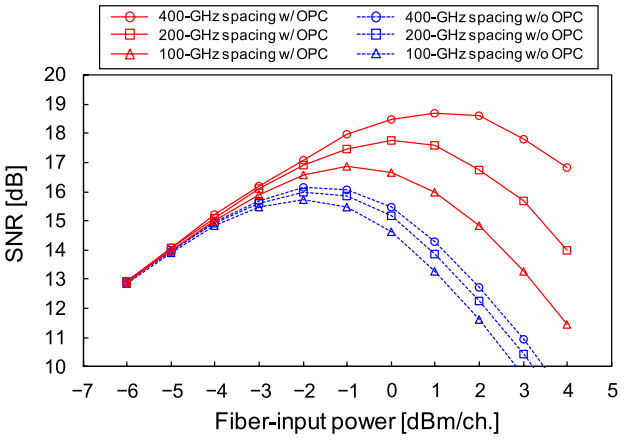

Fig. 3 Simulation results for SNR of center channel as function of fiber-input power with 3.0-ps/nm/km chromatic dispersion at 1550 nm.

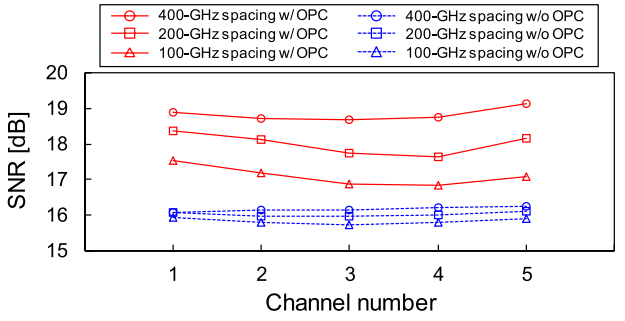

Fig. 4 Channel dependence of SNR at optimal fiber-input power with 3.0-ps/nm/km chromatic dispersion at 1550 nm.

the single-channel transmission due to the frequency shift of OPC is not that large in transmission over standard single-mode fibers (SMFs), which have a > 15-ps/nm/km CD [19]. These simulation results showed the channel dependence for the WDM transmission and NZ-DSF-like parameters. In the no-OPC cases, the SNR was slightly higher towards the outer channel. This is because there were fewer interference channels for XPM on the outside than on the inside. The SNR difference between channel 1 and 3 was 0.20 dB in the 100-GHz spacing. There was almost no channel dependence in the 400-GHz spacing because the influence of XPM was very small. In comparison, the OPC cases had a slightly greater channel dependence than no-OPC cases. There was an SNR difference of 0.68 dB with the 100-GHz spacing and 0.46 dB even with the 400-GHz spacing. This result suggests that OPC-assisted systems is sensitive for the XPM-induced noise.

Figure 5 shows the SNR of the center channel as a function of the local CD at 1550 nm. In the no-OPC cases, the SNR increased monotonically with the increase in the absolute value of CD due to the growth of the walk-off regardless of the channel spacing. The lowest peak was −0.5 ps/nm/km at which the CD was zero near the center frequency of the WDM signal. Under the zero-CD condition, the XPM had a particularly large impact due to the small walk-off, so the

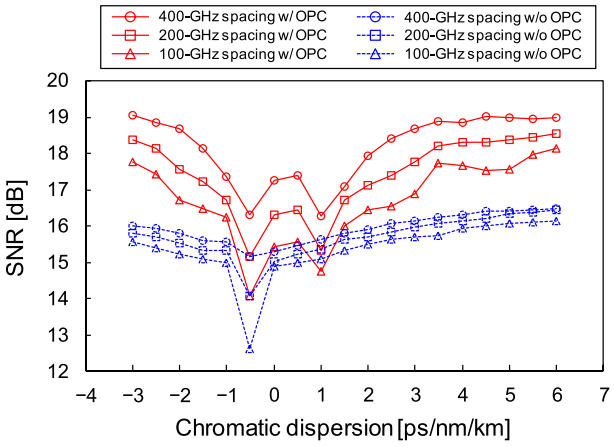

Fig. 5 Simulation results for SNR of center channel as function of local chromatic dispersion at 1550 nm.

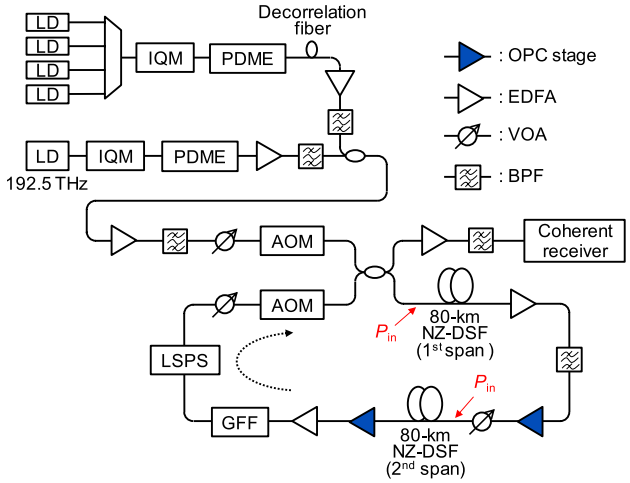

Fig. 6 Experimental setup for long-haul WDM transmission using PPLN-based OPC with 160-km NZ-DSF recirculation loop and 80-km amplifier spacing. Case without OPC are implemented by bypassing OPC stages. LD: laser diode, IQM: I/Q modulator, PDME: polarization-division multiplexing emulator, BPF: band-pass filter, VOA: variable optical attenuator, AOM: acousto-optic modulator-based optical switch, GFF: gain-flattening filter, LSPS: loop-synchronous polarization scrambler, P_{in}: fiber-input power.

SNR deteriorated with a narrower channel spacing. The SNR difference caused by the channel spacing gradually decreased with increase in CD, and there was almost no difference between 200-GHz and 400-GHz spacing in the region of > 5 ps/nm/km. In the OPC cases, the SNR was significantly degraded at two points, -0.5- and 1.0-ps/nm/km CD. The reason for the peak at -0.5 ps/nm/km was the same as that in the no-OPC case. 1.0 ps/nm/km was the value at which the local CD of the idler light frequency-shifted by OPC was almost zero. Therefore, there was no walk-off in the phase-conjugate-propagation section. This suggests that it is necessary to pay attention not only to the local CD of the original signal light but also to that of the phase-conjugated light in OPC-assisted systems. A nonlinear mitigation effect of OPC exceeding this impairment could not be obtained with the zero-CD condition for the idler light due to the power map asymmetry of lumped amplification, so the deterioration in SNR was considered to be remarkable. A similar deterioration was confirmed even in the 400-GHz spacing unlike the no-OPC case. These results show that the impact of XPM was greater in the transmission system using OPC than in the no-OPC systems.

From the above results, it was shown that the sensitivity for XPM was large in the transmission system using OPC. It was suggested that extending the channel spacing is more effective for OPC-assisted systems than conventional systems.

4. Experiment on Long-Haul WDM Transmission over NZ-DSF Using Inline EDFA with OPC

To experimentally verify the impact of channel spacing expansion on OPC-assisted systems, we conducted a lumped optical amplified five-channel WDM transmission experiments with an 80-km amplifier spacing. We used PPLN waveguides for OPC by DFG. This experiment examined the center channel in the WDM signal most degraded by XPM.

4.1 Experimental Setup

Figure 6 shows the experimental setup for long-haul WDM transmission with the PPLN-based OPC. The transmission line consisted of a 160-km NZ-DSF recirculating loop with an 80-km amplifier spacing. The phase-matching frequency of our PPLN waveguides were 194.0 THz. Five-WDM channels were implemented with a spacing of 100, 200, or 400 GHz. The channel under test (CUT) was the center channel at 192.5 THz regardless of the channel spacing. The optical carrier at 192.5 THz was modulated to Nyquist-pulse shaped 32-Gbaud DP-QPSK with a roll-off factor of 0.03. The interference WDM channels were simultaneously modulated in the same format as the CUT and decorrelated by passing through a 20-km SMF. The CUT and dummy channels were polarization-multiplexed by polarization-division-multiplexing emulators (PDMEs) with a 75-ns decorrelation delay and then combined with a 2×1 optical coupler. The input and output of the recirculation loop was controlled by acousto-optic modulator-based optical switches (AOMs) and a 2×2 optical coupler. The polarization state for each lap was randomly modulated by a loop-synchronous polarization scrambler (LSPS). The input power of each span was controlled to be equal by variable optical attenuators (VOAs) and inline EDFAs. Band-pass filters (BPFs) were used to eliminate amplified spontaneous emission (ASE) light in the unwanted band from optical amplifiers. A gain-flattening filter (GFF) was used to equalize the power spectrum of the amplified signal. In the OPC stage, signal light was converted to its conjugated light. The converted WDM signal was centered at 195.5 THz. Figure 7 shows the frequency dependence of the local CD in an NZ-DSF measured by a dispersion analyzer. The dispersion slope was 0.07 ps/nm^2/km. The CDs

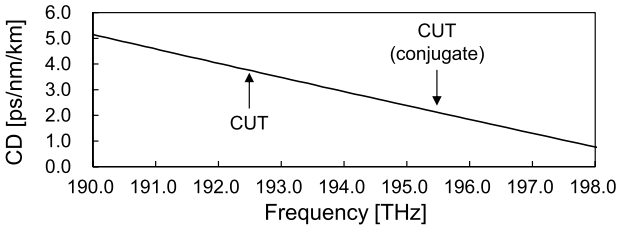

Fig. 7 Frequency dependence of CD in NZ-DSF used in experiment. CDs of channel under test (CUT) and its conjugate are 3.7 and 2.1 ps/nm/km, respectively.

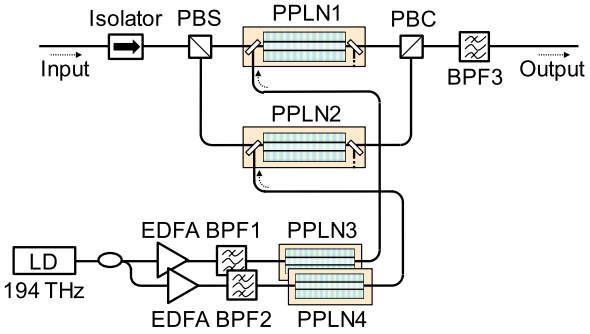

Fig. 8 Configuration of polarization-diverse OPC stage. BPF3 is filter that allows only idler components to pass through. PBS: polarization-beam splitter, PBC: polarization-beam combiner.

of the CUT and its conjugate were 3.7 and 2.1 ps/nm/km. The OPC stages were located at both ends of the 2nd span. Therefore, the phase-conjugated light centered at 195.5 THz propagated only during the 2nd span, and there was no change in the frequency allocation of WDM channels at each point in each lap. At the receiver side, the WDM signal was pre-amplified with an EDFA and the CUT was extracted using a BPF. The CUT was received by a dual-polarization coherent receiver. The received signal was demodulated using a 2×2 adaptive filter with pre-convergence using training symbols and tracking by the DD-LMS algorithm after CD compensation in the offline DSP. The CD of the received signal was estimated by a delay tap sampling estimation (DTSE) method with a 50-ps/nm resolution [20]. Similar to the above numerical simulations, the signal quality was evaluated by calculating the SNR on the basis of the variance in the signal after the symbol decision from the desired symbols.

Figure 8 shows the configuration of PPLN-based polarization-diverse OPC. The center frequency of the phase-matching of PPLN waveguides was 194.0 THz. The DFG in $\chi^{(2)}$-nonlinear media was driven by a pump light with the second harmonic (SH) of the center frequency. Each PPLN waveguide was used for phase conjugation by DFG and frequency up-conversion of pump light by SH generation (SHG). By using different PPLN waveguides for SHG and DFG, it is possible to suppress the unnecessary nonlinear optical process [21]. The pump light was amplified by a 1.5-μm-band EDFA and converted to SH light by SHG in PPLN3 or PPLN4. The input signal light was divided into two orthogonal polarization components by a polarization-beam splitter (PBS) after passing through an isolator. By passing through PPLN1 or PPLN2 with the SH pump, the input light was amplified while idler light was generated. The signal light and SH pump light were (de-)multiplexed by dichroic filters. Finally, the BPF3 extracted only idler light after combining orthogonal polarization components with a polarization-beam combiner (PBC). The gain of PPLN1 and PPLN2 was set to 10 dB from the PBS input to the PBC output. The losses of the BPFs in the 1st and 2nd OPC stages for rejecting original signals were 2.3 and 4.8 dB, respectively. Figure 9 shows the input and output spectra of the OPC stage before the 2nd span in each channel arrangement with a 0.1-nm resolution. It was confirmed that the conversion efficiency in each WDM channel was uniform within ±0.1 dB. The conversion efficiency was stable over time and did not affect the measurement of SNR. The OPC stages were inserted every 80 km so that the frequency of light entering each component would always be the same in each lap in order to make gain equalization easy. In an ideal configuration, the OPC should be inserted once every two spans even if it is the most frequently inserted. Therefore, the OSNR penalty for inserting the OPC in this setup was greater than in the ideal configuration.

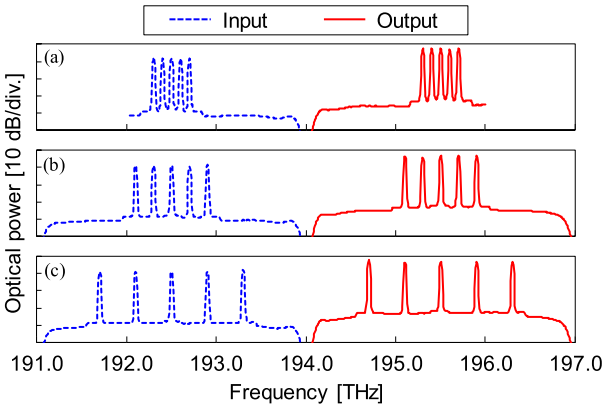

Fig. 9 Input and output spectra of 1st OPC stage (0.1-nm resolution). (a) 100-GHz, (b) 200-GHz, (c) 400-GHz spacing WDM signal.

4.2 Results and Discussion

Figure 10 shows the CD estimated by the DTSE method in offline receiver DSP. Without OPC, the CD accumulated at 525–550 ps/nm per lap which was in good agreement with the amount measured from the CD analyzer. With OPC, the accumulation of the CD was relaxed and was 150–175 ps/nm per lap. This residual CD was caused by the dispersion slope and the frequency shift by OPC. From this result, it was confirmed that periodic CD mitigation was performed by OPC.

Figure 11 shows the calculated SNR of the received signals after 960-km transmission as a function of the fiber-input power. In the no-OPC case, the nonlinear tolerance was slightly improved by extending the channel spacing. The amount of improvement between the 100-GHz spacing and

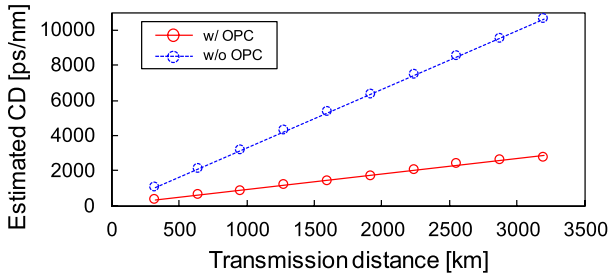

Fig. 10 Accumulated chromatic dispersion in received signal estimated by delay tap sampling estimation method as function of transmission distance in 400-GHz spacing cases.

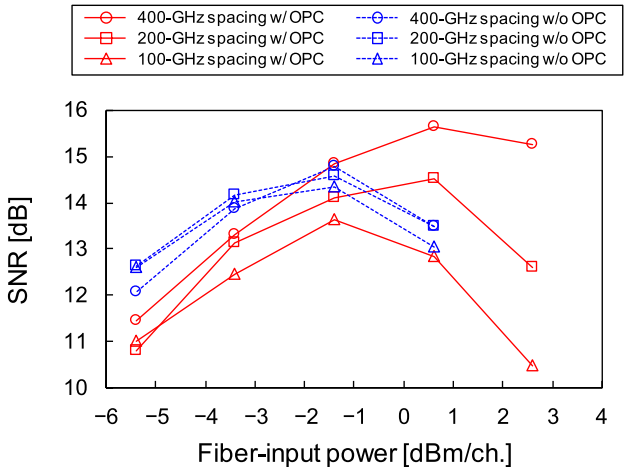

Fig. 11 SNR as function of fiber-input power after 12 × 80-km transmission.

400-GHz spacing was 0.6 dB at a −1.4-dBm input. In the case with OPC, the SNR changed significantly depending on the channel spacing unlike the no-OPC case. The SNR difference between the 100-GHz spacing and 400-GHz spacing was 2.0 dB. However, in the linear region at a −5.4-dBm input, there was a 1.5-dB penalty in contrast with the no-OPC cases due to the linear noise penalty caused by excessive loss from passing through the OPC stages. In the 200-GHz spacing, the optimal input power was improved by 2 dB, although there was no improvement in the maximum SNR in comparison with the no-OPC case due to the linear noise penalty. In the 400-GHz spacing, an SNR improvement exceeding the linear noise penalty was confirmed, and the maximum SNR was improved by 0.87 dB. The trend of the SNR and optimal power variances by OPC and the channel spacing were in good agreement with the simulation results. In the nonlinear region at a 2.6-dBm input in the 100-GHz and 200-GHz spacing cases, the tracking behavior of the adaptive filter for nonlinear distortion significantly degraded the SNR. In this experiment, the linear noise penalty due to the insertion of OPC was excessive because the number of OPC insertions was higher than really needed for ease of setup. In particular, the OPC after the 2nd span was placed before the EDFA and thus directly degraded the link NF. The linear noise penalty can be reduced by setting the OPC once every two

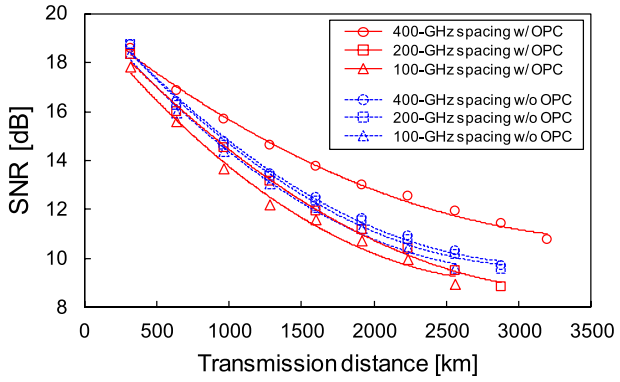

Fig. 12 SNR as function of transmission distance. Lines indicate second-order polynomial approximation.

spans as with the above simulation setup while maintaining nonlinearity-mitigation efficiency. It is also conceivable to further reduce the number of OPC insertions at the expense of increasing the random-walk length of non-deterministic nonlinear phase noise.

Figure 12 shows the SNR as a function of the transmission distance at the optimal input power. In the no-OPC cases, the SNR improved slightly as the channel spacing increased. With the 100-GHz and 200-GHz spacing, since the nonlinear compensation effect was smaller than the deterioration of the OSNR, SNR improvement with OPC could not be confirmed. However, with the 400-GHz spacing, the longer the transmission distance, the greater the amount of improvement in the SNR. The reason for this is that the wide channel spacing reduced the effects of XPM-induced noise, and the strong compensation effect of OPC for SPM-induced noise became apparent. Comparing in the region where the SNR was less than 11 dB, an extension of >1,000 km by OPC was shown. From the above experimental results, it was shown that the spacing of optic-electric-optic conversion can be extended by widening the channel interval even in the case where the OPC is inserted most frequently.

5. Conclusion

We numerically and experimentally investigated the impact of channel spacing in a WDM signal on nonlinear signal distortion in OPC-assisted transmission with a lumped optical amplified NZ-DSF link. Simulation results showed that the SNR was greatly improved by expanding the channel spacing in OPC-assisted systems, which are sensitive for XPM, compared with no-OPC systems. In numerical simulations with the SSFM, the nonlinear mitigation effect of OPC was improved by about 1.4 dB by expanding the channel spacing from 100 GHz to 400 GHz. We also experimentally demonstrated five-channel WDM long-haul transmission using PPLN-based polarization-diverse OPC. Similar to the simulation results, the performance in transmission using OPC was highly dependent on the channel spacing. In the 100-GHz and 200-GHz spacing cases, an improvement in the signal quality could not be confirmed with the

OSNR penalty due to the insertion of OPC. In contrast, in the 400-GHz spacing case, an improvement exceeding the OSNR penalty was obtained, and an extension of >1,000 km in transmission distance was confirmed. These results suggest that it is necessary to design the channel spacing more carefully on the basis of the required number of channels and the transmission performance to be achieved in OPC-assisted systems.

References

[1] T. Kawasaki, M. Inami, Y. Sakakura, D. Shimazaki, M. Horiguchi, and K. Koda, "Development of 100-Gbit/s packet transport system," NTT Technical Review, vol.13, no.3, pp.1–7, 2015.
[2] A.D. Ellis, M.E. McCarthy, M.A.Z. Al Khateeb, M. Sorokina, and N.J. Doran, "Performance limits in optical communications due to fiber nonlinearity," Adv. Opt. Photon., vol.9, no.3, pp.429–503, 2017.
[3] E. Ip, "Nonlinear compensation using backpropagation for polarization-multiplexed transmission," J. Lightwave Technol., vol.28, no.6, pp.939–950, 2010.
[4] F.P. Guiomar, J.D. Reis, A.L. Teixeira, and A.N. Pinto, "Mitigation of intra-channel nonlinearities using a frequency-domain Volterra series equalizer," Opt. Express, vol.20, no.2, pp.1360–1369, 2012.
[5] O. Sidelnikov, A. Redyuk, S. Sygletos, M. Fedoruk, and S. Turitsyn, "Advanced convolutional neural networks for nonlinearity mitigation in long-haul WDM transmission systems," J. Lightwave Technol., vol.39, no.8, pp.2397–2406, 2021.
[6] A. Yariv, D. Fekete, and D.M. Pepper, "Compensation for channel dispersion by nonlinear optical phase conjugation," Opt. Lett., vol.4, no.2, pp.52–54, 1979.
[7] P. Minzioni and A. Schiffini, "Unifying theory of compensation techniques for intrachannel nonlinear effects," Opt. Express, vol.13, no.21, pp.8460–8468, 2005.
[8] T. Umeki, T. Kazama, A. Sano, K. Shibahara, K. Suzuki, M. Abe, H. Takenouchi, and Y. Miyamoto, "Simultaneous nonlinearity mitigation in 92 × 180-Gbit/s PDM-16QAM transmission over 3840 km using PPLN-based guard-band-less optical phase conjugation," Opt. Express, vol.24, no.15, pp.16945–16951, 2016.
[9] T. Kobayashi, T. Umeki, R. Kasahara, H. Yamazaki, M. Nagatani, H. Wakita, H. Takenouchi, and Y. Miyamoto "96-Gbaud PDM-8QAM single channel transmission over 9,600 km by nonlinear tolerance enhancement using PPLN-based optical phase conjugation," Proc. Opt. Fiber Commun. Conf. (OFC), Th3E.4, March 2018.
[10] A.D. Ellis, M. Tan, Md A. Iqbal, M.A.Z. Al-Khateeb, V. Gordienko, G.S. Mondaca, S. Fabbri, M.F.C. Stephens, M.E. McCarthy, A. Perentos, I.D. Phillips, D. Lavery, G. Liga, R. Maher, P. Harper, N. Doran, S.K. Turitsyn, S. Sygletos, and P. Bayvel, "4 Tb/s transmission reach enhancement using 10×400 Gb/s super-channels and polarization insensitive dual band optical phase conjugation," J. Lightwave Technol., vol.34, no.8, pp.1717–1723, 2016.
[11] M.A.Z. Al-Khateeb, M.E. McCarthy, C. Sanchez, and A.D. Ellis, "Nonlinearity compensation using optical phase conjugation deployed in discretely amplified transmission systems," Opt. Express, vol.26, no.18, pp.23945–23959, 2018.
[12] P. Minzioni, V. Pusino, I. Cristiani, L. Marazzi, M. Martinelli, C. Langrock, M.M. Fejer, and V. Degiorgio, "Optical phase conjugation in phase-modulated transmission systems: Experimental comparison of different nonlinearity-compensation methods," Opt. Express, vol.18, no.17, pp.18119–18124, 2010.
[13] A.A.I. Ali, M. Al-Khateeb, T. Zhang, F. Ferreira, and A. Ellis, "Enhanced nonlinearity compensation efficiency of optical phase conjugation system," Proc. Opt. Fiber Commun. Conf. (OFC), Th2A.11, March 2019.
[14] K.P. Ho, "Error probability of DPSK signals with cross-phase modulation induced nonlinear phase noise," J. Lightwave Technol., vol.10, no.2, pp.421–427, 2004.
[15] M.E. McCarthy, M.A.Z. Al Kahteeb, F.M. Ferreira, and A.D. Ellis, "PMD tolerant nonlinear compensation using in-line phase conjugation," Opt. Express, vol.24, no.4, pp.3385–3392, 2016.
[16] M.A.Z. Al-Khateeb, M. McCarthy, C. Sanchez, and A.D. Ellis, "Effect of second order signal-noise interactions in nonlinearity compensated optical transmission systems," Opt. Lett., vol.41, no.8, pp.1849–1852, 2016.
[17] E.F. Mateo, F. Yaman, and G. Li, "Efficient compensation of inter-channel nonlinear effects via digital backward propagation in WDM optical transmission," Opt. Express, vol.18, no.14, pp.15144–15154, 2010.
[18] Q. Zhang and M.I. Hayee, "Symmetrized split-step Fourier scheme to control global simulation accuracy in fiber-optic communication systems," J. Lightwave Technol., vol.26, no.2, pp.302–315, 2008.
[19] F. Da Ros, M. Lillieholm, M.P. Yankov, P. Guan, H. Hu, S. Forchhammer, M. Galili, and L.K. Oxenløwe, "Impact of signal-conjugate wavelength shift on optical phase conjugation-based transmission of QAM signals," Proc. Eur. Conf. Opt. Commun. (ECOC), P1.SC4.66, Sept. 2017.
[20] D. Wang, C. Lu, A.P.T. Lau, and S. He, "Adaptive chromatic dispersion compensation for coherent communication systems using delay-tap sampling technique," Photon. Technol. Lett., vol.23, no.14, pp.1016–1018, 2011.
[21] T. Kazama, T. Umeki, M. Abe, K. Enbutsu, Y. Miyamoto, and H. Takenouchi, "Low-parametric-crosstalk phase-sensitive amplifier for guard-band-less DWDM signal using PPLN waveguides," J. Lightwave Technol., vol.35, no.4, pp.755–761, 2016.

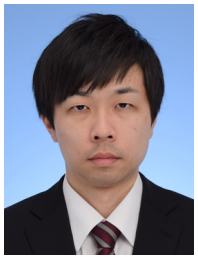

Shimpei Shimizu received the B.E. degree in engineering and the M.E. degree in information science and technology from Hokkaido University, Sapporo, Japan, in 2016 and 2018, respectively. He joined the NTT Network Innovation Laboratories, Yokosuka, Japan, in 2018. He is a member of the Institute of Electronics, Information and Communication Engineers (IEICE) of Japan and the IEEE Photonics Society.

Takayuki Kobayashi received the B.E., M.E., and Dr. Eng. degrees from Waseda University, Tokyo, Japan, in 2004, 2006, and 2019, respectively. In April 2006, he joined the NTT Network Innovation Laboratories, Yokosuka, Japan, where he was engaged in the research on high-speed and high-capacity digital coherent transmission systems. In April 2014, he moved to the NTT Access Network Service Systems Laboratories, Yokosuka, and was engaged in 5G mobile optical network systems. Since July 2016, he moved back to the NTT Network Innovation Laboratories and has been working on high-capacity optical transmission systems. His current research interests are long-haul optical transmission systems employing spectrally efficient modulation formats enhanced by digital and optical signal processing. He is a member of the Institute of Electronics, Information and Communication Engineers (IEICE) of Japan. He has been served as a Technical Program Committee (TPC) Member of the Electrical Subsystems' Category for the Optical Fiber Communication Conference (OFC) from 2016 to 2018. He has been serving as a TPC Member of the "Point-to-Point Optical Transmission" Category for the European Conference on Optical Communication (ECOC) since 2018.

Takeshi Umeki received the B.S. degree in physics from Gakusyuin University, Tokyo, Japan, in 2002, and the M.S. degree in physics and the Ph.D. degree in nonlinear optics from The University of Tokyo, Tokyo, in 2004 and 2014, respectively. He joined the NTT Photonics Laboratories, Atsugi, Japan, in 2004, since then he has been involved in research on nonlinear optical devices based on periodically poled $LiNbO_3$ waveguides. He is a member of the Japan Society of Applied Physics (JSAP), the Institute of Electronics, Information, and Communication Engineers (IEICE), and the IEEE/Photonics Society.

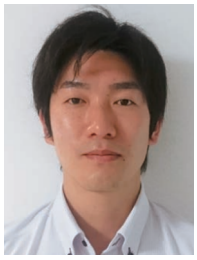

Takushi Kazama received the B.S. and M.S. degrees in electrical engineering from The University of Tokyo, Tokyo, Japan, in 2009 and 2011, respectively. In 2011, he joined the NTT Device Technology Laboratories, Japan, where he has been engaged in research on nonlinear optical devices based on periodically poled $LiNbO_3$ waveguides. He is a member of the Institute of Electronics, Information, and Communication Engineers of Japan (IEICE) and the Japan Society of Applied Physics (JSAP).

Koji Enbutsu received the B.E. and M.E. degrees in electronics engineering from Hokkaido University, Sapporo, Japan, in 1994 and 1996, respectively. In 1996, he joined the NTT Opto-Electronics Laboratories, Japan, where he engaged in research on organic optical waveguides for optical communications and electro-optic crystals and their devices. In 2007, he moved to the NTT Access Services Network System Laboratories, where he engaged in research on optical fiber testing and monitoring. He is a member of the Institute of Electronics, Information, and Communication Engineers (IEICE) and the Japan Society of Applied Physics (JSAP).

Ryoichi Kasahara received the B.S. degree from The University of Electro-Communications, Tokyo, Japan, in 1995, and the M.S. degree from Tohoku University, Sendai, Japan, in 1997. In 1997, he joined the NTT Opto-Electronics Laboratories, Japan, where he was involved in research on silica-based planar lightwave circuits (PLCs), including thermo-optic switches and arrayed-waveguide grating multiplexers, and integrated optoelectrical receiver modules. He is currently with the NTT Device Technology Laboratories, Japan, where he has been involved in the research and development of the fabrication technologies of optical dielectric waveguide devices. He is a Senior Member of the Institute of Electronics, Information, and Communication Engineers of Japan (IEICE) and a member of the Japan Society of Applied Physics (JSAP).

Yutaka Miyamoto received the B.E. and M.E. degrees in electrical engineering from Waseda University, Tokyo, Japan, in 1986 and 1988, respectively, and the Dr. Eng. degree in electrical engineering from Tokyo University, Tokyo, in 2016. He joined the NTT Transmission Systems Laboratories, Yokosuka, Japan, in 1988, where he was engaged in the research and development of highspeed optical communications systems including the 10-Gbit/s first terrestrial optical transmission system (FA-10G) using erbium-doped fiber amplifiers (EDFA) inline repeaters. He was with the NTT Electronics Technology Corporation, Yokohama, Japan, from 1995 to 1997, where he was engaged in the planning and product development of high-speed optical module at the data rate of 10 Gb/s and beyond. Since 1997, he has been with the NTT Network Innovation Laboratories, Yokosuka, where he has contributed to the research and development of optical transport technologies based on 40/100/400-Gbit/s channel and beyond. He is currently an NTT Fellow and the Director of the Innovative Photonic Network Research Center, NTT Network Innovation Laboratories, where he has been investigating and promoting the future scalable optical transport network with the Pbit/s-class capacity based on innovative transport technologies such as digital signal processing, space division multiplexing, and cutting-edge integrated devices for photonic preprocessing. He is a fellow of the Institute of Electronics, Information and Communication Engineers (IEICE).